NEAR INFRARED RESPONSE OF AMORPHOUS SILICON DETECTOR GROWN WITH MICROCOMPENSATED ABSORBER LAYER

D. CAPUTO*, G. DE CESARE*, A. NASCETTI*, F. PALMA*, M. TUCCI**
* Department of Electronic Engineering, University of Rome "La Sapienza", via Eudossiana 18, 00184 Rome (Italy)
** ENEA, Research Centre, Località Granatello, 80055, Portici, Napoli, (Italy)

ABSTRACT

In this work we demonstrate that radiation up to 2 μm induces photocurrent in a single junction amorphous silicon structure at room temperature. The absorber layer is a microcompensated film deposited using very low concentrations of dopant species. Device operation is based on optical excitation of thermal generated carriers from trap states toward valence and conduction band in the high electric field region of the structure. Transient and frequency response under different bias voltages and illuminations conditions are presented. The possibility to use the infrared sensor in low bit rate communication systems has been demostrated by including our detector in a front-end system and measuring its frequency responce.

Quantum efficiency measurement have been reproduced with a numerical model, able to take into account sub-band gap absorption into single films. Model results indicate the presence of a large valence band tail and a high number of dangling bonds and shallow defects ascribed to the presence of dopant atoms.

INTRODUCTION

Single junction p-i-n amorphous silicon (a-Si:H) structures have been extensively used as solar cells, with quantum efficiency response up to 750 nm or 900 nm when the absorber region is an intrinsic amorphous silicon layer or an intrinsic amorphous silicon-germanium layer, respectively [1, 2, 3]. Constant photocurrent method and photothermal deflection spectroscopy showed that the presence of defects in the forbidden gap allowed to obtain photocurrent response up to 1500 nm in intrinsic a-Si:H films. The first detection of radiation up to 2400 nm by a-Si:H a p-i-n diode, operating under forward bias conditions at low temperature (198 K), has been reported by Wind and Müller [4].

More recently, it has been demonstrated the possibility to achieve near and medium infrared detection at room temperature by using single junction a-Si:H structure with microcompensated absorber zone, whose operation is based on the transitions between the high number of defect density present in this material and the extended states [5, 6]. Here, we present a detailed investigation of the near infrared responce of this device focusing the attention on the detection mechanism and on its transient and frequency responce. Altough near infrared a-Si:H detectors are orders of magnitude slower than detectors based on the III-V technology, they could represent a complementary approach, because a-Si:H technology, which requires low deposition temperature, is suitable for almost any kind of substrate and, in particular, it is compatible with silicon IC and integrated optics technology [7].

EXPERIMENTAL RESULTS

On a transparent conductive oxide coated glass the deposition of the amorphous layers is performed as the following steps:
1) 300 Å thick p-doped amorphous silicon carbide layer;
2) 7000 Å thick microcompensated amorphous silicon layer;
3) 500 Å thick n-doped amorphous silicon layer.
The microcompensated zone has been deposited with 0.25 ppm of PH_3 and 18 ppm of B_2H_6 in the gas mixture. This low dopant concentrations justifies the name of this layer. The front electrode was aluminum deposited by evaporation and then shaped as a thin finger grating, with spacing of 50 μm. The area of the fabricated devices ranged from 25 mm^2 to 1 cm^2.

Mat. Res. Soc. Symp. Proc. Vol. 557 © 1999 Materials Research Society

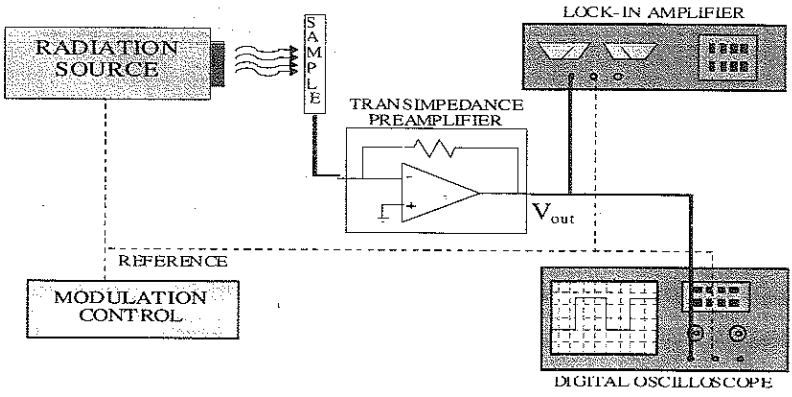

Figure 1. Measurement set-up used in the transient, frequency and quantum efficiency response. The utilized radiation sources were a LED emitting at 950 nm, a Nd:Yag laser emitting at 1.32 μm and a Nernst ceramic element filtered with a monochromator in the range 800 nm - 4.5 μm.

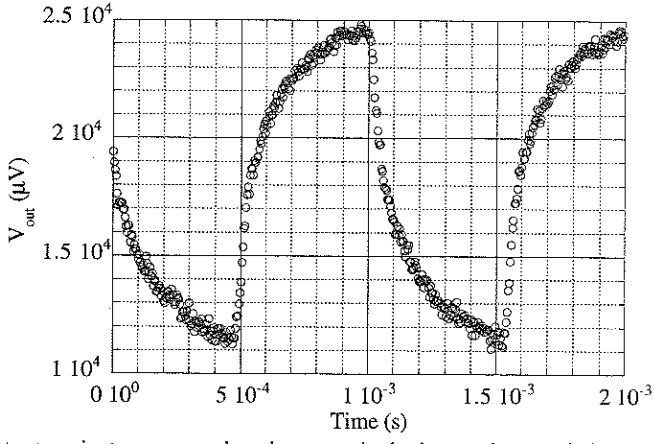

Figure 2. Detector transient response when the power inpinging on the sample is equal to 10mW. The radiation comes from a a Nd:Yag laser emitting at 1.32 μm. The shape of the waveformindicates that a photocurrent signal is detected.

Data reported in this paper refer to 25 mm^2 devices. The radiation is impinging from the aluminum grid, to avoid absorption of the IR radiation by the glass substrate.

Transient response characterization

The measurement set-up for the transient response is reported in figure 1. The radiation source is a Nd:Yag laser emitting at 1.32 μm. The transimpedance amplifier has been realized with a three stages preamplifier using low noise electronic components and having a gain of 10^6 V/A. The output signal coming from the transimpedance amplifier is read with a EG&G 5210 lock-in amplifier and is simultaneously displayed on a 9100 LeCroy digital oscilloscope.

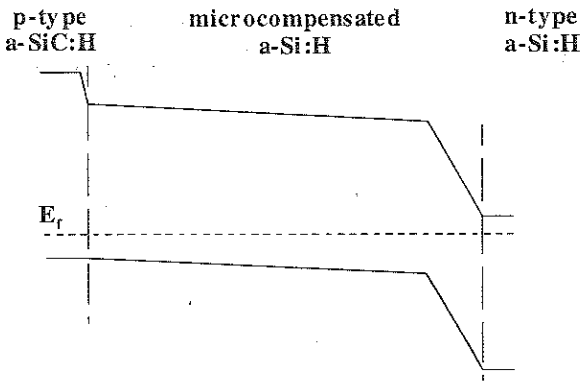

Figure 3. Band diagram inferred from quantum efficiency measurements in the visible range.

In figure 2 the transient response, with incident power equal to 10mW, is reported. The period of the radiation was 1ms with 50% duty cycle. The shape of the waveform indicates that a photocurrent signal is detected. The slow speed response, observable in fidure 2, indicates that inour device photoconduction is strongly affected by trapping mechanisms. Since the energy of the incident photons (0.94 eV) is lower than the band gap of a-Si:H (1.72 eV), the observed signal has to involve sub-gap transitions. On the other side, photocurrent in a junction implies transport of both type of carriers, and then the incident radiation induces transitions between localized and extended states to generate free holes and free electrons. In particular, photocurrent in the device is due to the combined effect of photo-induced and thermal induced transitions from localized states toward valence and conduction band. From quantum efficiency measurements in the visible range with light impinging on the p-side or on the n-side [6], it has beeen inferred that the band diagram of the device is the one reported in figure 3. It can be seen that the microcompensated layer behaves as p-type region near the p-doped a-SiC:H layer and that the high electric field region exists only close to the n-doped zone. Since minority carriers have a very low diffusion length in highly defective amorphous materials as are doped films, photogeneration is effective only in the region near the microcompensated-n interface.

Frequency characterization

In figure 4 detector response as a function of a 950nm LED modulation frequency is shown. The different curves refer to different average incident power achieved by applying different bias voltage to the LED. For each curve the amplitude of the modulated signal is kept constant. It can be observed that frequency response depends on the light intensity. In particular, the higher is the light intensity, the higher the cut-off frequency. This behavior can be explained taking into account that an increase of the bias light intensity causes occupation of defects in the forbidden gap and then a decrease of the number of states which are effective in the trapping process.

Results of figure 4 have been obtained by keeping the detector in short circuit conditions. A further frequency characterization has been performed applying a forward bias voltage to the sensor. Results are reported in figure 5. An increase of the photocurrent is observed as the forward bias level is increased. A similar behavior has been found by Wind and Müller on a-Si:H p-i-n diodes at 198 K, who ascribed the effect to IR induced re-excitation of excess carriers trapped in the band tails, during forward bias injection of charge carriers, toward extended states.

Applying a reverse bias voltage to the device, only a sligthly increase of the frequency responce is achieved, due to the presence of the high defect density in the absorber layer, which screens off the electric field due to the applied voltage.

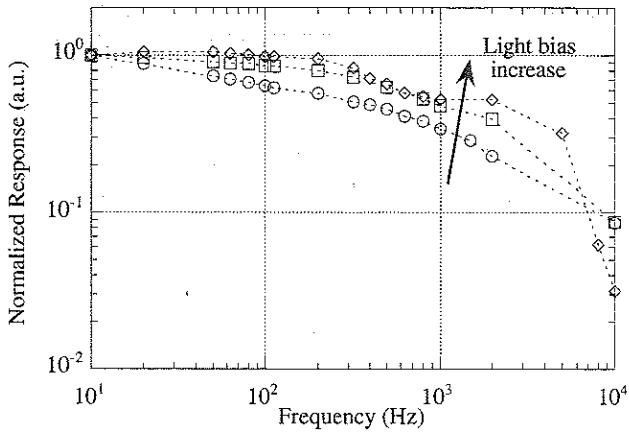

Figure 4. Normalized photocurrent versus frequency of a radiation incident from a 950nm LED. For each curve the amplitude of the modulated signal is kept constant.

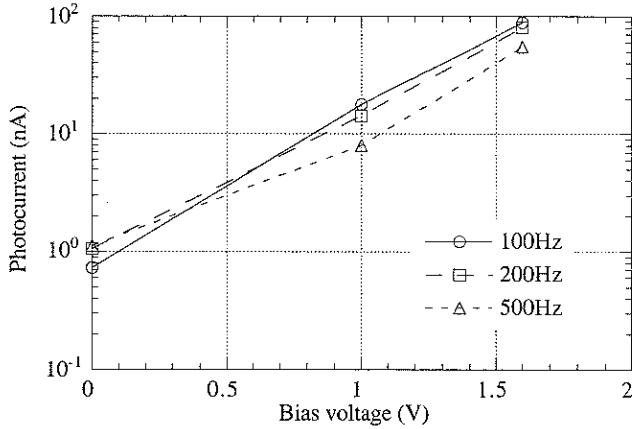

Figure 5. Photocurrent signal as function of the forward bias voltage to the detector. Different curves refer to different modulation frequencies of the incident radiation.

Results of figure 4 and 5 show that the frequency responce of our detector is quite poor (not higher than 500 Hz). In order to overcome this limitation we included our detector in a front-end system realized with discrete electronic component. The operation of the whole system is based on pole-zero compensation and allows to obtain a bandwidth of 100 kHz. The measured frequency response allows the use of the detector in communication system at low bit rate (up to 125 kbit/sec) [8], as remote control systems and IR interface for hand-pocket calculators.

QUANTUM EFFICIENCY CHARACTERIZATION AND MODELING

A better insight in the detection mechanism can be deduced by measuring the sensor response at different wavelengths as reported in figure 6. In this case the radiation source was a Nernst ceramic element filtered by a monochromator in the range 800 nm – 2 μm. Photocurrent values are read by the lock-in amplifier. Altough the photocurrent signal decays almost exponentially, the detector response is detectable up to 2 μm. Performing the same measurement on a p-i-n device, where the absorber layer is an intrinsic film, the photocurrent is always beyond the noise introduced by the measurement set-up.

In order to have quantitative informations on the defect distribution involved in the detection mechanism the quantum efficiency response has been reproduced by a numerical model of sub-band gap absorption in single films. The model includes both thermal and optical induced transitions. The non-equilibrium condition is simulated by assuming excess values of electron and hole densities , which determine lectron and hole quasi Fermi levels. Exponential band tails and Guassian distributions of dangling bonds (DB) and charged defects (CD) have been used. Occupancy function for the tail states were derived using the Shockley-Read-Hall recombination theory, while the occupancy function for DB and CD were derived taking into account their three possible states of occupancy. Solid line in figure 6 is the model reproduction of the experimental quantum efficiency data. An good agreement is achieved. Modeled results have been obtained by using a slope of 950 K for the valence band tail, DB distributions positioned at 0.80 eV and 0.95 eV above the valence band with densities equal to 10^{17} cm^{-3} and $5 \cdot 10^{17}$ cm^{-3}, and CD distribution lying at 0.45 eV above the valence band with density equal to $5 \cdot 10^{18}$ cm^{-3}. The ratio of capture cross section for charged and neutral states are 1 and 100 for DB and CD, respectively. Transitions involved in the investigated wavelength range do not allow to achieve informations on states lying less than 0.6 eV below the conduction band. The high values of modeled density of states can be ascribed to the effect of dopant impurities which dramatically increase the number of band tail states and both deep and shallow defect states [9, 10, 11].

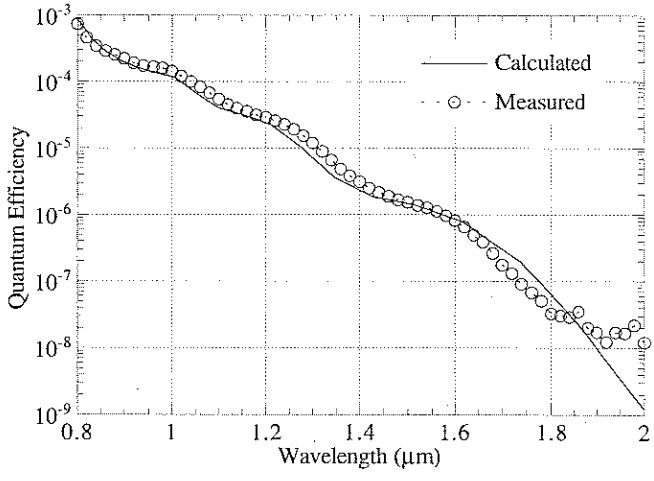

Figure 6. Quantum efficiency response obtained by using as radiation source a Nernst ceramic element filtered by a monochromator

CONCLUSIONS

Room temperature photocurrent caused by near infrared radiation has been observed in a single junction a-Si:H based on microcompensated amorphous silicon layer. Sensor response has been characterized in detail by transient, frequency and quantum efficiency measurents. Modeling of quantum efficiency response by a numerical model of amorphous silicon films suggests the presence of a high number of defects both around mid-gap and in shallow position. An appropriate design of a front-end circuit allows to use the detector in communication systems up to 125 kbit/sec.

REFERENCES

1. S. Guha, J. Yang, A. Banerjee, T. Glatfelter, K. Hoffman, S. R. Ovshinsky, M.Izu, H. C. Ovshinsky, X. Deng in *Amorphous Silicon Technology*, edited by E.A. Schiff, M. Hack, A. Madan, M. Powell and A. Matsuda (Mat. Res. Soc. Symp. Proc. **336**, Pittsburgh 1994), p. 645-655.

2. P.P. Deimel, B.Heimhofer, G. Krötz, H.J. Lilenhof, J. Wind, G. Müller, E. Voegs, IEEE Photon. Technol. Lett., **2**, 499, (1990).

3. Y.K.Fang, S.B. Hwang, K.H. Chen, C.R. Liu, L.C. Kuo, IEEE Trans. Electron Devices, **39**, 1350, (1992).

4.J. Wind, G. Müller, Appl. Phys. Lett. **59**, 956, (1991).

5. D. Caputo, G. de Cesare, A. Nascetti, F. Palma, M. Petri, Appl. Phys. Lett., **72**, 1229, (1998).

6. D.Caputo, A.Nascetti, F.Palma, IEEE Photon. Tech. Lett., **10** , 1147, (1998).

7. H. Fisher, J. Schulte, P. Rieve, M. Bohm in *Amorphous Silicon Technology*, edited by E.A. Schiff, M. Hack, A. Madan, M. Powell and A. Matsuda (Mat. Res. Soc. Symp. Proc. 336, Pittsburgh 1994), p. 867-872.

8. A. Buchwald, K. Martin, Integrated Fiber-Optics Receivers, (Kluwer Academic Publishers, Boston, 1995), p. 168.

9 . R.A. Street, D.K. Biegelsen, J.C. Knights, Phys. Rev. B, **24**, 969, (1981).

10 . W.B. Jackson, N.M. Amer, Phys. Rev. B, **25**, 5559, (1982).

11. D. Caputo, G. de Cesare, F. Palma, M. Tucci, C. Minarini, E. Terzini, J. Non-Cryst. Solids, **227-230**, 380, (1998).